JTTEE5 11:542-550

Peer Reviewed

An Analysis of the Cold Spray Process and Its Coatings

T. Stoltenhoff, H. Kreye, and H.J. Richter

(Submitted 13 May 2001; in revised form 12 November 2001)

In this study, computational fluid dynamics (CFD) and extensive spray tests were performed for detailed analyses of the cold spray process. The modeling of the gas and particle flow field for different nozzle geometries and process parameters in correlation with the results of the experiments reveal that adhesion only occurs when the powder particles exceed a critical impact velocity that is specific to the spray material. For spherical copper powder with low oxygen content, the critical velocity was determined to be about 570 m/s. With nitrogen as the process gas and particle grain sizes from 5-25 µm, deposition efficiencies of more than 70% were achieved. The cold sprayed coatings show negligible porosity and oxygen contents comparable to the initial powder feedstock. Therefore, properties such as the electrical conductivity at room temperature correspond to those of the bulk material. The methods presented here can also be applied to develop strategies for cold spraying of other materials such as zinc, stainless steel, or nickel-based super-alloys.

Keywords cold spraying, composite coatings, computational fluid dynamics, copper coatings, MCrAlY coatings, stainless steel coatings

1. Introduction

In flame, arc, and plasma spraying it is important that the spray material in the form of wire or fine powder particles melts completely. In contrast, in the high velocity oxygen fuel (HVOF) spray process, partial melting of the powder is already sufficient to achieve a high-quality coating. This is because in the latter process the particle velocities before impact on the substrate are considerably higher, thus plastic deformation of the particles occurs upon impact even if the particles are still solid. In the new process, cold spraying, the development of even higher particle velocities has been rigorously continued with a simultaneously reduced and controlled heat input into the spray material and the substrate. Here the gas temperature is well below the melting temperature of the material so that the particles do not melt at all in the gas, but considerable particle deformation upon impact occurs, resulting in good bond strength of the coating. The low temperatures of the process also permit spraying onto substrates containing temperature-sensitive materials.

Cold spray was developed in the mid-1980s by chance at the Institute of Theoretical and Applied Mechanics, part of the Siberian Division of the Russian Academy of Science in Novosibirsk. Experiments were performed in a supersonic wind tunnel with very small particles entrained in the high velocity gas stream. The erosive behavior of this particle-laden flow on an object in the wind tunnel was studied. It was discovered that above a particular minimum particle velocity, the abrasion caused by the particles changes to adhesion of the particles, i.e., a coating is formed on the object. This effect is enhanced by an increase in gas temperature. This process, now called cold spraying, has been patented.[1,2] It was presented for the first time in the United States in 1995 at a major thermal spray conference.[3]

T. Stoltenhoff and **H. Kreye,** Universitaet der Bundeswehr Hamburg, 22043 Hamburg, Germany; and **H.J. Richter,** Thayer School of Engineering, Dartmouth College, Hanover, NH 30755. Contact e-mail: Horst.J.Richter@dartmouth.edu.

2. Principles of the Cold Spray Process and Experimental Setup

In the cold spray process, a gas is accelerated to supersonic velocity in a de'Laval-type nozzle, i.e., a converging-diverging nozzle. The coating material is injected into the gas stream in powder form at the inlet of the nozzle, accelerated by the gas in the nozzle, and propelled toward the substrate to be coated. Above a certain particle velocity, which is characteristic for each respective powder material and its properties, the particles form a dense and solid adhesive coating on the substrate surface. Upon impact the particles must undergo sufficient deformation to adhere to the surface. The gas is heated to temperatures up to 923 K (650 °C) before entering the nozzle. This increases the particle temperature and velocity, and thus assists deformation upon impact. However, the gas temperature at the inlet is clearly below the melting temperature of the coating material, which means the particles cannot be melted in the gas jet. In comparison to other thermal spray processes, drawbacks connected with melting, such as oxidation and undesirable phase transformations, can be avoided with the cold spray process.

The basic principle of the process is illustrated in Fig. 1. Nitrogen is favored as the process gas, which can be used to spray most materials suitable for this application without causing oxidation. The nitrogen is supplied from liquid gas tanks. The use of nitrogen-helium (He) mixtures or He alone results in higher gas velocities for the same inlet conditions and nozzle geometry, which also produces higher particle velocities. Therefore, it is possible to spray materials that require higher kinetic energy. However, because of the prohibitive price of He, its use is reserved for special applications.

The cold spray installation, set up at the University of the Federal Armed Forces in Hamburg, Germany, operates at maxi-

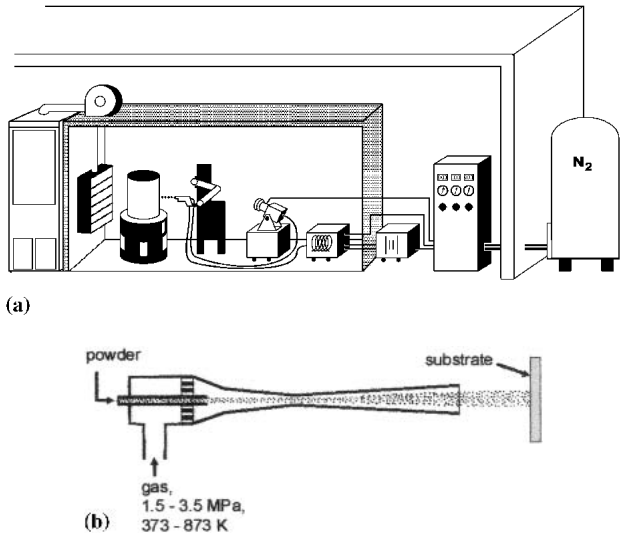

Fig. 1 **(a)** Assembly of a cold spray installation; **(b)** principle of cold gas spraying

mum gas stagnation pressures of 3.5 MPa (35 bar) and gas temperatures of up to 923 K at the inlet of the nozzle. These parameters can be regulated via a control unit. Furthermore, the control unit includes sensors for process monitoring and several safety modules. The gas is heated to a preset temperature in a coil of an electric resistance heated tube. The power supply is provided by a welding transformer, which is integrated into the unit. The gas heater is connected to the inlet of the nozzle via a flexible hose coupling. The powder is injected along the axis of the nozzle, coming from a high-pressure powder disk feeder. The carrier gas in the feeder is nitrogen. The gas pressure and gas temperature of the process gas are measured at the nozzle prechamber.

The noise level is markedly lower than that of HVOF spraying. Despite this, the cold spray process is placed in a soundproof chamber with an air-extraction and exhaust-air cleaning system.

3. Fluid Dynamic Concepts of the Cold Spray Process

The particles impinge on the substrate with a certain velocity and either cause a plastic deformation or an erosion of the substrate, and they either adhere to the substrate or bounce back. Adhesion does not occur until a critical particle velocity has been exceeded; a velocity specific to the particle material, which is most likely also dependent on the particle temperature at the time of impact. It is possible to obtain these values from detailed computations of the flow of gas and particles in the nozzle and the free jet. These computations, which have been performed in this work, describe the influence of the nozzle geometry and all significant process parameters such as the process gas used, its pressure and temperature, particle type and size, and influence of powder feed rate and spray distance on the particle velocity and temperature. Such computations serve to provide a better understanding of the process. Moreover, they reduce the time and effort invested in experiments to optimize the coating properties.

For basic initial results of gas velocity and temperature in the nozzle, it is advantageous to consider the gas flow to be ideal, isentropic, and one-dimensional. Thus, heat and friction losses are not considered. Under these simplified conditions, the changes of state are merely functions of the local Mach number and the isentropic coefficient κ:

$$\frac{p}{p_0} - f(\mathrm{Ma},\kappa); \quad \frac{\rho}{\rho_0} = f(\mathrm{Ma},\kappa); \quad \frac{T}{T_0} = f(\mathrm{Ma},\kappa) \qquad \text{(Eq 1)}$$

The subscript 0 represents the upstream stagnation condition of the gas.

The isentropic coefficient κ is 1.67 for monatomic gases such as He and approximately 1.4 for diatomic gases such as nitrogen, but in the latter case the coefficient is a weak function of the temperature, as is considered here.[4,5] The local Mach number is defined as

$$\mathrm{Ma} = \frac{v}{a}, \quad \text{with } a = \sqrt{\kappa R T} \qquad \text{(Eq 2)}$$

With the help of these correlations, the Mach number, the velocity, and all of the properties of state are calculated for each cross-section A along the nozzle:

$$\frac{A}{A*} = \mathrm{Ma}\left[\frac{2}{\kappa+1} + \frac{\kappa-1}{\kappa+1}\mathrm{Ma}^2\right]^{-\frac{\kappa+1}{2(\kappa-1)}} \qquad \text{(Eq 3)}$$

$A*$ is the minimum cross-section (throat) of the nozzle.

Using the computational fluid dynamics (CFD) code FLUENT (Fluent, Inc., Lebanon, NH), the flow field, which is divided into a few hundred thousand finite volume cells, is evaluated and heat conduction, turbulence, or frictional losses are taken into account. The Navier-Stokes equations and energy equations, as well as further scalar equations, e.g., for two-phase flow, are solved for each cell. Because the flow is turbulent, appropriate turbulence models have to be chosen for the flow field. In this case, the Reynolds stress model (RSM) is used. The computations are extended to the environment of the nozzle and to the free jet because intermixture of environmental air results in changing velocities and temperatures of the free jet and the particles. Furthermore, the gas flow in the vicinity of the substrate is of considerable importance.

The advantages of these computations are production of detailed information about the gas temperature and velocity fields, and about particle trajectories, temperatures, and velocities throughout the nozzle and the free jet. The disadvantages are the extensive computer resources and computational time required. Thus, for first estimates the ideal one-dimensional calculations have been performed as described above.

As soon as gas velocity and temperature are known, particle acceleration and particle heat transfer can be calculated. Acceleration and deceleration of the particles are considered to be only functions of the drag force, thus:

$$\rho_\mathrm{p} \frac{\pi d_\mathrm{p}^3}{6} \frac{Dv_\mathrm{p}}{Dt} = \frac{1}{2} C_\mathrm{D} \rho_\mathrm{g} \frac{\pi d_\mathrm{p}^2}{4} (v_\mathrm{g} - v_\mathrm{p}) |v_\mathrm{g} - v_\mathrm{p}| \qquad \text{(Eq 4)}$$

where ρ_g and ρ_p are the densities of the gas and particle; v_g and v_p are the gas and particle velocity, respectively; and d_p is the diameter and C_D the drag coefficient of the particle. The gravitational force is neglected here because the residence time of the particles in the flow is very short. Furthermore, the particle concentration in the flow is so small that particle-particle interaction can be neglected. The mass concentration of particles in the gas flow is only about 3% and the highest volume concentration is approximately 0.008%.

For a constant drag coefficient the particle acceleration is proportional to the gas density and to the square of the relative velocity, and inversely proportional to the particle density and particle diameter. The relative velocity between gas and particle can be greater than the local sound velocity, thus a shock will form in front of the particle. In this case, the standard formula for C_D, which is according to Wallis [6] and is only a function of the Reynolds number, is no longer valid. It is necessary to introduce a drag coefficient, which is also a function of the Mach number, because the shock in front of the particle has a considerable influence on the particle acceleration. According to Walsh,[7] the drag coefficient is therefore a function of the Reynolds number and the particle Mach number Ma_p

$$C_D = f(Ma_p, Re_p) \quad \text{(Eq 5)}$$

with

$$Ma_p = \frac{|v_g - v_p|}{\sqrt{\kappa R T_g}} \quad \text{(Eq 6)}$$

and

$$Re_p = \frac{\rho_g |v_g - v_p| d_p}{\mu_g} \quad \text{(Eq 7)}$$

The heat transfer between gas and particle as a result of the high Mach number flow is obtained by introducing a modified Nusselt number:[8]

$$Nu = 2 + 0.44\, Re_p^{0.5}\, Pr^{0.333} \exp(0.1 + 0.872\, Ma_p) \quad \text{(Eq 8)}$$

However, this is only valid for $Ma_p > 0.24$ and $T_g > T_p$. In all other cases the general Nusselt number—independent of the Mach number—is used:

$$Nu = 2 + 0.6\, Re_p^{0.5}\, Pr^{0.333} \quad \text{(Eq 9)}$$

Because of the very high heat conduction coefficient of copper (Cu), it is assumed that the particle has a uniform temperature at any time. This is true if the following condition for the Biot number is valid:

$$Bi = \frac{h d_p}{k_p} < 0.1 \quad \text{(Eq 10)}$$

where h is the gas heat transfer coefficient and k_p is the heat conductivity of the spray material.

4. Velocity and Temperature of the Particles

The FLUENT code was used for the evaluation of a nozzle with an exit to minimum (throat) cross-section ratio of $A_E/A* = 9$, which corresponds to a Mach number of 3.8. These computations provide information about the changes of temperature and velocity for the gas (g) and the particles (p) throughout the nozzle and the free jet to the substrate S, as illustrated in Fig. 2. The calculations are for nitrogen as the process gas with an inlet stagnation pressure of $p_0 = 2.5$ MPa and a temperature of $T_0 = 593$ K and for a Cu particle 15 μm in diameter (p15).

Most of the gas acceleration takes place in the area of the nozzle throat and in the first third of the divergent nozzle section. Here the gas has already reached 90% of its exit velocity. At the same time, the gas temperature decreases to values below room temperature. The irregular changes in the gas velocity and temperature of the free jet are the result of shocks, which form because the pressure of this supersonic jet is not the same as the pressure in the environment. At the exit from the nozzle the gas is overexpanded, thus its pressure is lower than the environmental pressure.

The gas velocity increases substantially close to the throat of the nozzle and in the first part of the divergent nozzle section, as mentioned previously. The particle velocity increases significantly only later in the nozzle (Fig. 2). For most of the free jet, the gas velocity is higher than the particle velocity. Thus, an acceleration of the particles continues to take place there as well. Along the convergent section of the nozzle the gas temperature decreases to about 80% of the value of the gas inlet temperature, but its velocity is slow, thus the residence time of the particles is relatively long. Therefore, particles heat up in this section correspondingly fast. The particles have a higher temperature than the gas in the diverging section of the nozzle, and approaching the nozzle exit the particles cool noticeably, but retain overall a higher temperature than the gas.

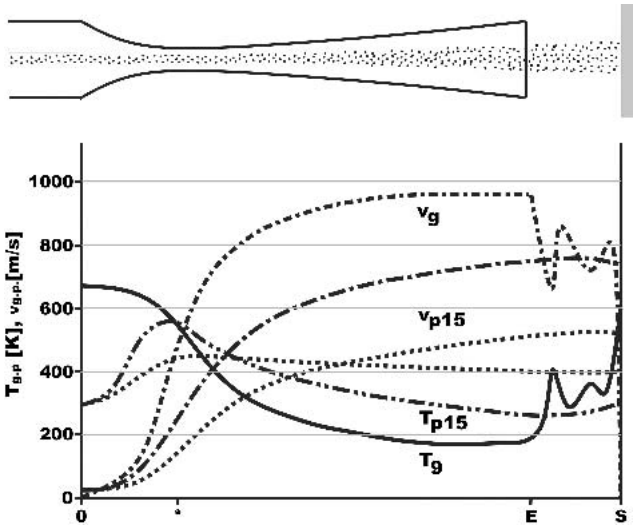

Fig. 2 Temperature and velocity development along the nozzle axis for nitrogen as the process gas (g) and a 15 μm Cu particle (p15), $T_0 = 593$ K, $p_0 = 2.5$ MPa

Figure 3 shows the influence of various process parameters on the velocity and temperature of the particles at the nozzle exit. Figure 3(a) and (b) is based on the relatively simple one-dimensional isentropic calculations. In this example, nitrogen is the process gas and Cu particles are used. Starting from a typical parameter setting for the gas of p_0 = 2.5 MPa and T_0 = 593 K, and a uniform particle diameter of d_p = 15 μm, it can be demonstrated to what extent the variation of gas inlet pressure or gas inlet temperature affects the velocity and temperature of the particles at the exit of the nozzle (Fig. 3a,b). Accordingly, the particle velocity can be increased by increasing the gas pressure as well as the gas temperature. Although the increase in gas pressure hardly influences the particle temperature, the increase in gas temperature also leads to a substantial temperature increase of the particles and thus assists their ability to deform upon impact.

Furthermore, in Fig. 3(c) the nozzle exit Cu particle velocity and temperature of different size particles are shown for the typical parameter setting for the gas of p_0 = 2.5 MPa and temperature of T_0 = 593 K. To reach a minimum particle velocity of, for example, 570 m/s, it is essential that the particles in the powder are restricted to a small size range. For Cu this means particle sizes only smaller than about 20 μm in diameter. A very high particle velocity can be achieved with particles smaller than 5 μm. However, because of their low inertia, such small particles are easily deflected before they reach the substrate as a result of the existing radial gas jet flow field in the vicinity of the substrate.

In Fig. 3(d), the particle velocity and temperature development for 15 μm diameter Cu particles is shown as a function of spray distance. Even though the computations indicate only a small variation of the particle velocity, the experiments show that the coating quality decreases if the spray distance exceeds 50 mm. Apparently, the entrainment of the environmental air into the free jet is not sufficiently considered in the calculations.

5. Experimental Evaluation of the Process and the Coatings for the Example of Cu Particles

Spray tests were carried out with a Cu powder of a particle size range from 5-25 μm and the coatings were studied using

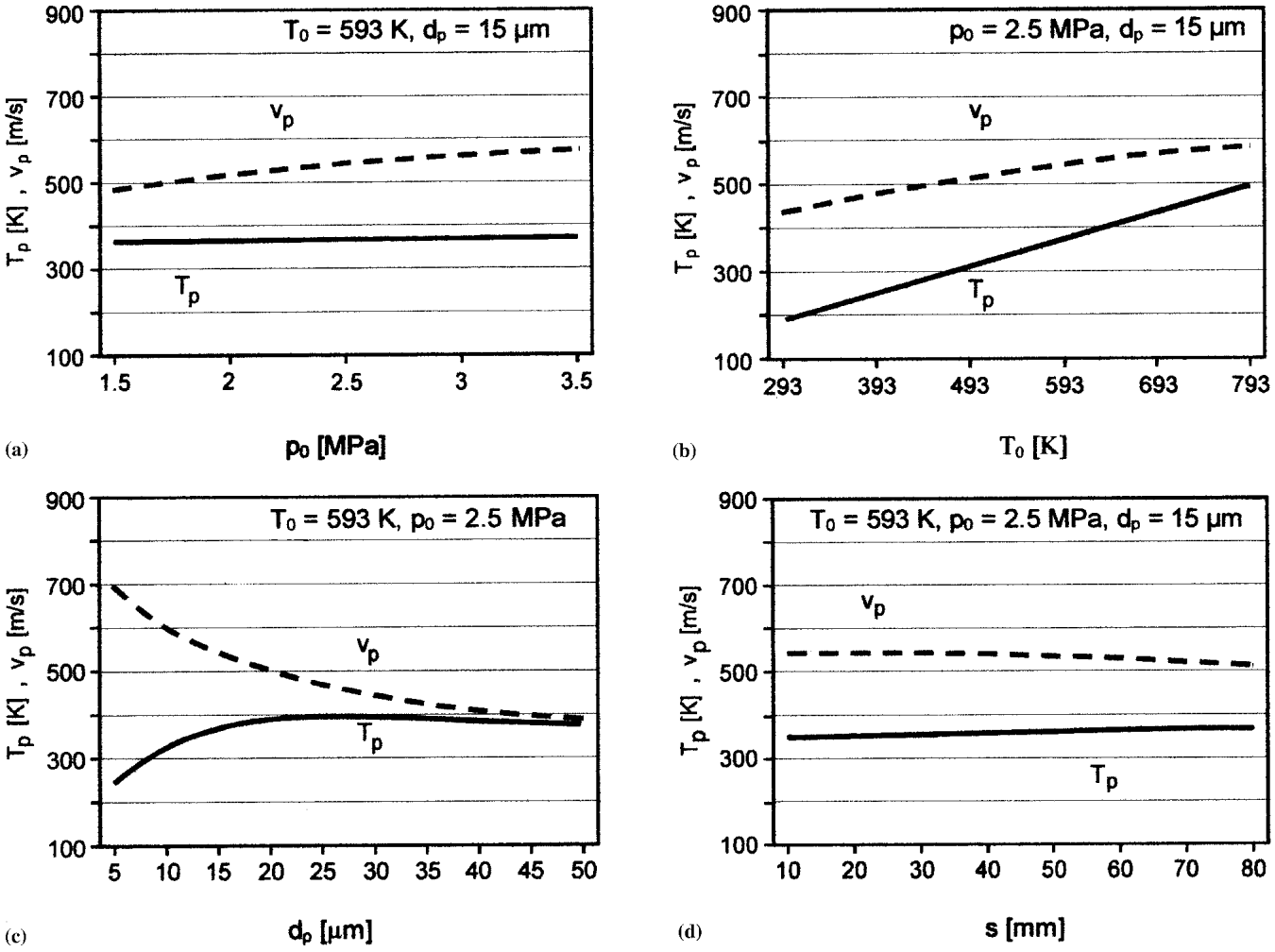

Fig. 3 Temperature and velocity of Cu particles at the nozzle exit as a function of **(a)** the gas inlet pressure p_0, **(b)** the gas inlet temperature T_0, and **(c)** the particle diameter d_p. **(d)** Particle temperature and velocity as a function of the spray distance s

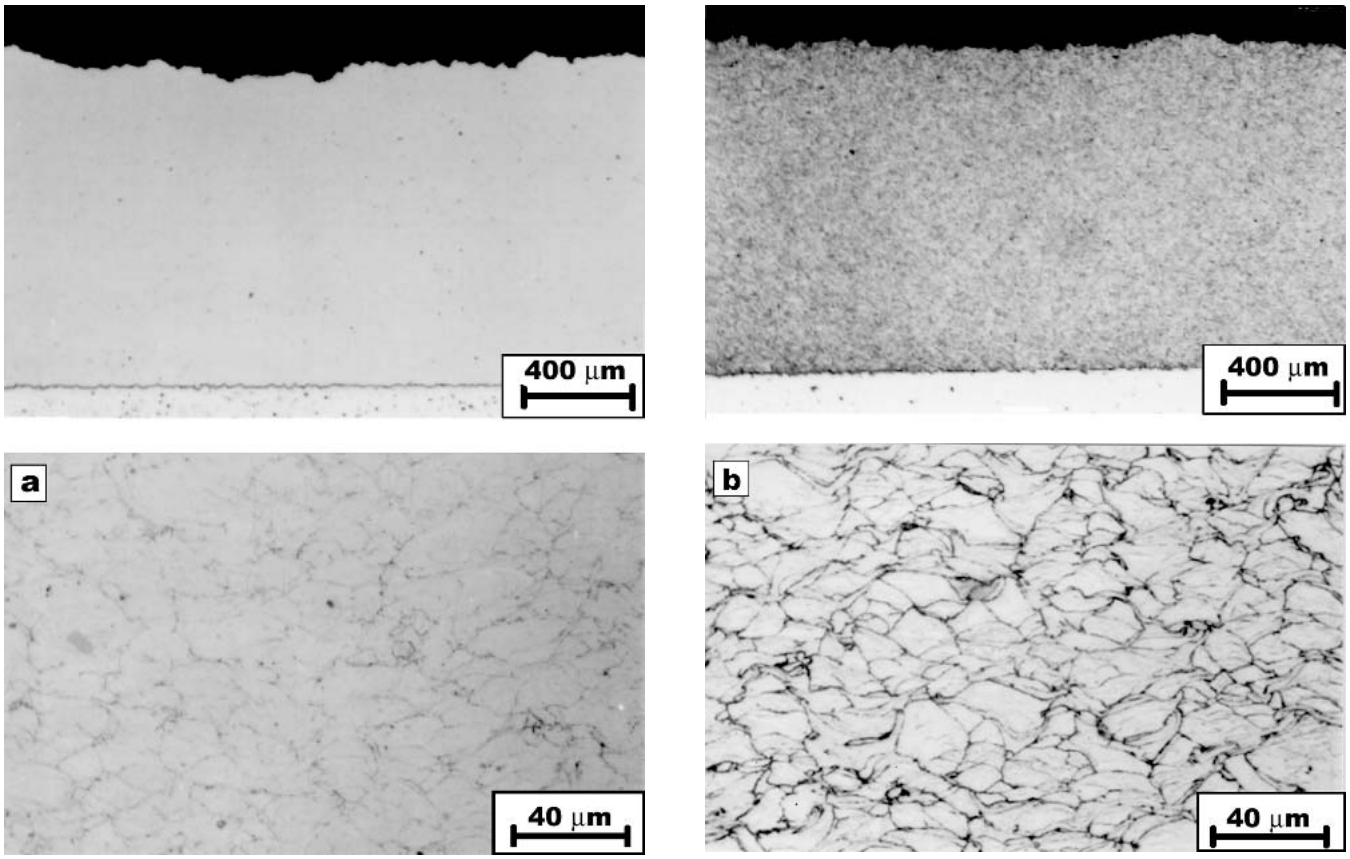

Fig. 4 OM of the cross-section of a cold sprayed Cu coating: **(a)** polished, **(b)** etched

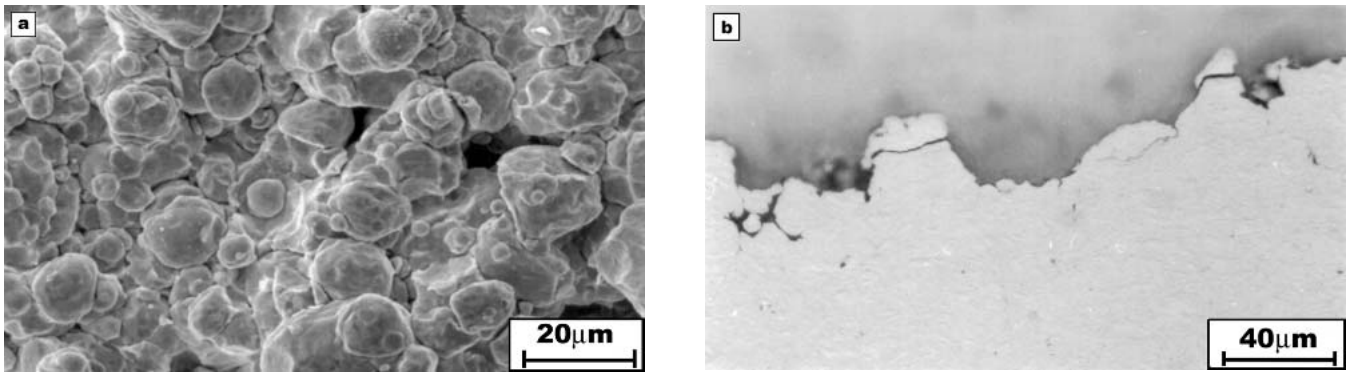

Fig. 5 **(a)** SEM of the surface of a cold sprayed Cu coating. **(b)** OM of the cross section near the coating surface

metallurgical methods. The process parameters were chosen based on the calculations in Sections 3 and 4. Nitrogen was used as the process gas. The flow rate was between 75 and 80 Nm^3/h. Here a nozzle with a cross-section ratio of $A_E/A* = 9$ and a minimum (throat) diameter of 2.7 mm was used. The stagnation gas pressure was 2.5 MPa, the gas inlet temperature was 593 K, the powder-feed rate was 3 kg/h, and the spray distance was 30 mm. Figure 4 shows optical micrographs (OM) of such a Cu coating. With a transverse sweep rate speed of the substrate of 125 mm/s and a line spacing of 1.7 mm, a thickness of 200-230 µm per layer was deposited. The deposition efficiency was 72%. The thickness of the coating illustrated here is about 1.1 mm.

In comparison to thermal spray coatings, these coatings are very dense and low in oxide content. Microstructure images show no evidence of pores. Differences in the coating density compared with solid Cu can only be determined using leak tests in which a vacuum of 10^{-12} mbar is produced on one side of the coating and in which the opposite side is filled with He. A coating with a thickness of 5.5 mm yielded a leak rate of only 10^{-10} mbar l/s, which roughly corresponds to the requirements for high-vacuum components. A section of this coating is shown in Fig. 5. Figure 5(a) shows a scanning electron micrograph (SEM) of the coating surface and Fig. 5(b) displays an OM of the cross section close to the coating surface. The oxygen content

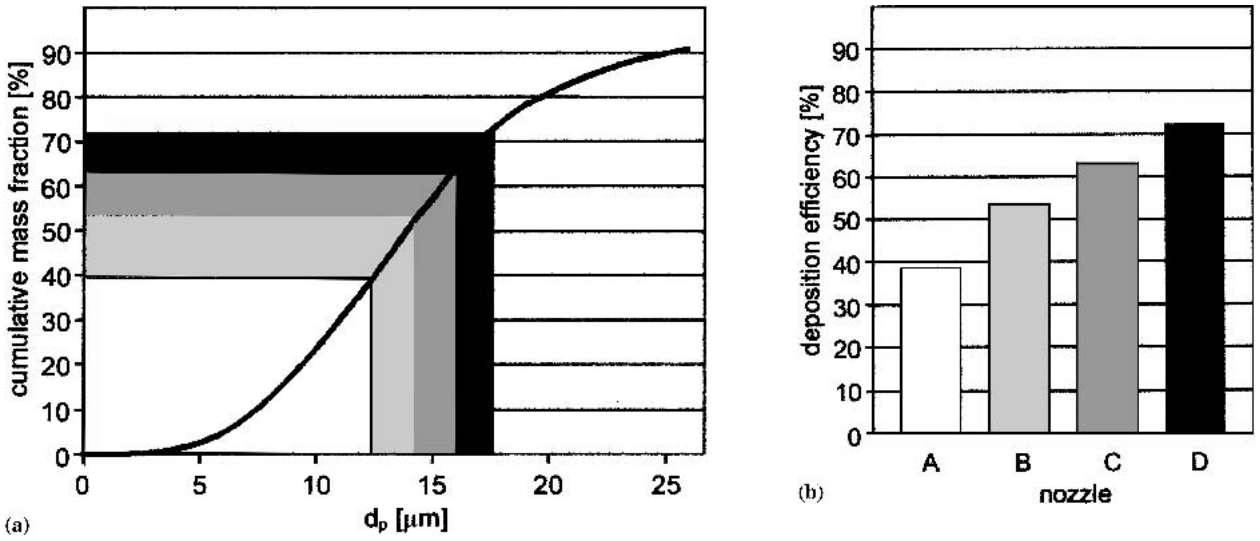

Fig. 6 **(a)** Particle size distribution of the experimental Cu powder. **(b)** Deposition efficiency for cold spraying of Cu with four different nozzles

of the coating of 0.1 wt.%, as determined by chemical analyses, corresponds to that of the powder. Absorption of oxygen during the spray process therefore did not take place, which is to be expected because nitrogen was the process gas and the spray distance was very short. Furthermore, the particle temperatures were low.

The hardness measurements produced values of 140 up to 160 HVO.1, which corresponds to the hardness of Cu severely deformed by cold rolling. However, when the coating is annealed, the hardness decreases considerably, but less than with deformed Cu. The high hardness of the coating is due to the high density of dislocations formed during the high velocity impact of the particles. Different from cold rolled material, the sprayed particles contain a high density of lattice defects such as vacancies and interstitial atoms. Upon heating, these defects form dislocation loops, which are thermally quite stable and retard the recrystallization of the deformed structure. Therefore, it is most likely that the slow decrease of hardness of the cold sprayed material is related to the high density of vacancies and interstitial atoms in the coating, as sprayed (see Ref. 9).

The coating was sprayed onto an aluminum substrate. The bond strength measurements have been performed according to the European standard EN582. The values determined for the coating range were from 35-40 MPa. Electrical resistance measurements of the coatings yielded 0.019 ohm · mm^2/m at 20 °C. This corresponds to 90% of the electrical conductivity of pure Cu (International Annealed Copper Standard). In contrast, Cu coatings sprayed with arc, plasma, or HVOF have only about 30% of the electrical conductivity of pure Cu (see Ref. 10).

Comparison of the OMs of the etched coatings in Fig. 4 with similar coatings produced in thermal spraying shows that in cold spraying the particles do not deform as much upon impact with the substrate. Microstructure images taken near the coating surface and the top view of the coating, illustrated in Fig. 5, show that in each case the last particle layer is not very dense. Here evidently, the subsequent particles impinge on the coating and produce a high density. Some type of microforging takes place.

It is informative to compare the cold spray process with the process of explosive welding. In both processes the collision velocities and geometries are quiet similar. Because it is well known that bonding in explosive welding requires a critical impact velocity, as described in Kreye et al.,[11] we assume that a

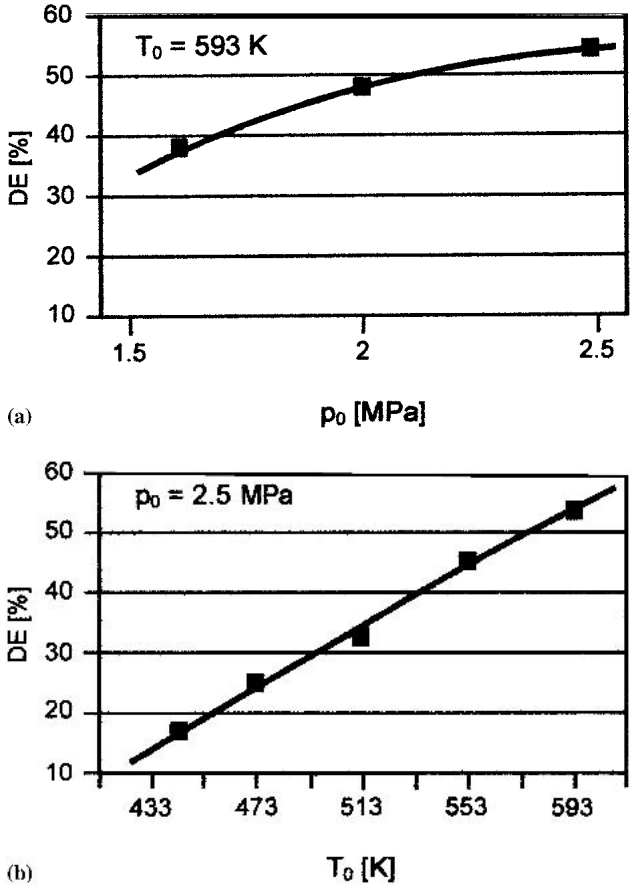

Fig. 7 Influence of **(a)** gas pressure and **(b)** gas temperature on the deposition efficiency. Cu-powder from 5-25 µm, spray distance 30 mm, standard nozzle B

critical velocity also exists in the cold spray process. Thus, when spraying with a powder of a particular particle size distribution, only those particles adhere that, because of their small size and therefore higher velocity, exceed this critical value. Therefore, the cumulative mass fraction of these particles determines the deposition efficiency. A typical particle size distribution of Cu powder is represented in Fig. 6(a).

These concepts of the cold spray process were developed from spray tests with various nozzle geometries. Four different type nozzles were built: A, B, C, and D. These had different throat diameters, and different contours and lengths in the divergent nozzle section. In nozzle A, the expansion ratio (i.e., the exit cross section divided by the throat cross section) is 6. Furthermore, the divergent section is conical. Nozzle B has the same length and contour of the divergent section but the expansion ratio is 9. In nozzle C, the divergent section is bell-shaped and lengthened by a factor of 1.5 with respect to nozzle A. Nozzle D is a modified version of nozzle B with a bell-shaped divergent

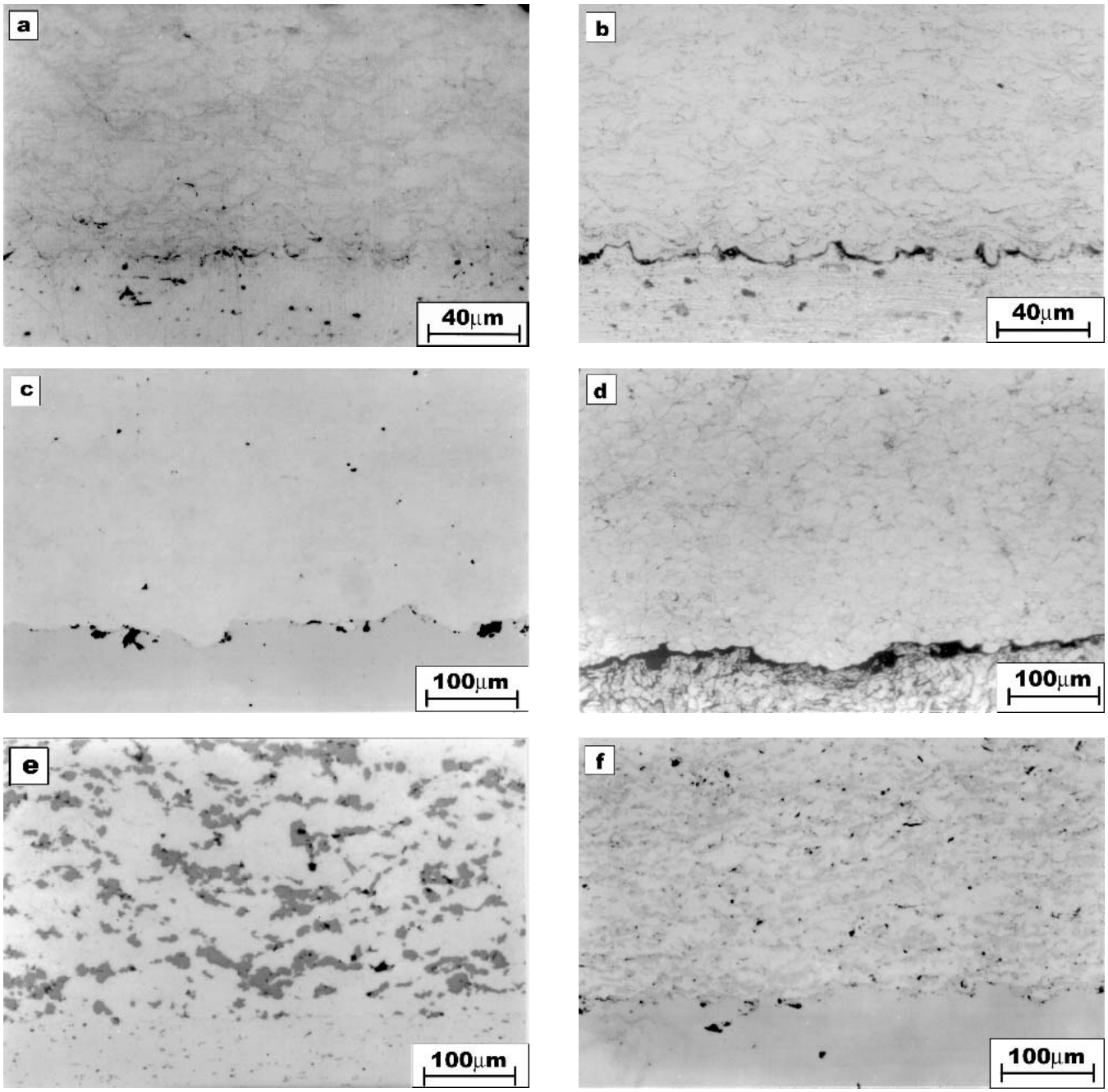

Fig. 8 OMs of the cross-section of a cold sprayed zinc coating on aluminum substrate **(a)** polished; **(b)** etched, 316L coating on carbon steel substrate; **(c)** polished; **(d)** etched, Al-Ti composite coating on aluminum substrate; **(e)** polished; and Cr_3C_2-NiCr composite coating on carbon steel substrate **(f)** polished

section, which is lengthened by a factor of 1.8. All nozzles were operated with the same parameter settings. The deposition efficiencies displayed in Fig. 6(b) are the results from the experiments.

By using both diagrams, i.e., Fig. 6(a) and (b), the maximum diameters of those particles, which adhere to the surface, can be determined. Then with the help of the FLUENT code the particle velocities for these maximum particle diameters were calculated immediately before impact on the substrate to produce the experimental spray distance. Remarkably, for all four nozzles the critical velocity is close to 570 m/s. If one considers the results strictly, the determined critical velocity is valid for the particular powder and parameter settings used in this work only. Additional experiments indicate that there are additional factors affecting the critical velocity, e.g., the oxygen content, alloying elements, and microstructure of the spray material.

Dense Cu coatings with low oxide content (Fig. 4) can be achieved in a relatively wide gas pressure and temperature range at the nozzle inlet. These process parameters have a strong influence on the gas and particle velocity and temperature, and therefore, the deposition efficiency, as can be seen in Fig. 7(a) and (b) respectively. However, the optimum parameters for spraying Cu have been determined to 593 K gas inlet temperature and 2.5 MPa gas inlet pressure. Indeed, the critical velocity value of 570 m/s, which has been calculated for optimum parameter settings, seems to decrease with increasing particle temperatures and thus the deposition efficiency would increase, too. However, because of nozzle plugging, higher gas temperatures, and therefore particle temperatures, are not practicable so far.

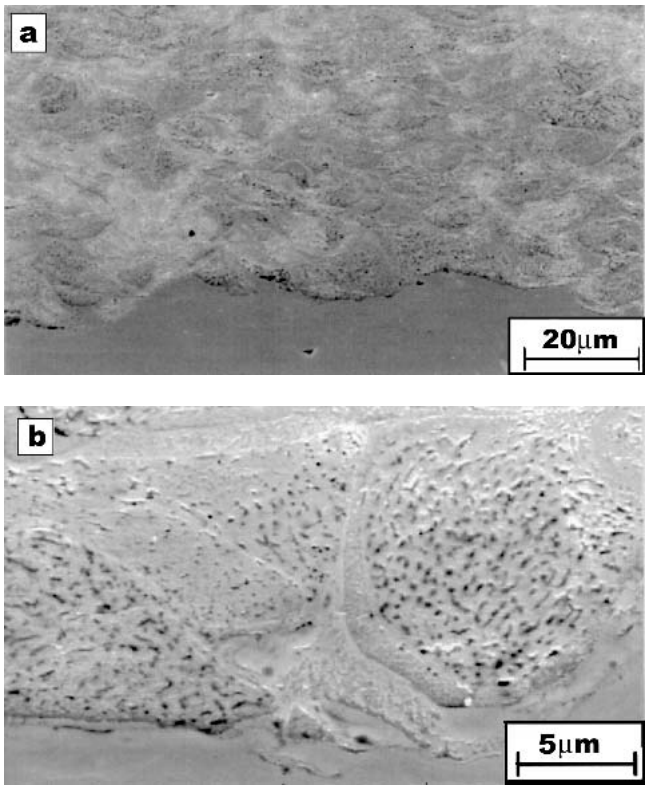

Fig. 9 Different scale SEMs of the cross section of a cold sprayed MCrAlY coating

6. Other Cold Spray Applications

The above analyses and experiments dealt with Cu particles. The analyses were concerned with the study of the influence of process parameter variations on the deposition efficiency and microstructure of the coatings. This knowledge can also be transferred to other metallic spray materials. Figure 8 shows examples of coatings of zinc, stainless steel 316 L, a composite of aluminum and titanium, and a composite of chromium carbide and nickel chromium, which can also be produced at gas inlet temperatures similar to the half of the melting temperature, in Kelvin, of the respective material.

Materials that have melting temperatures above 2300 K, such as niobium, require higher particle impact velocities. This is also true for materials with an ordered crystal lattice, which are difficult to deform plastically even at elevated temperatures, such as MCrAlY. With such materials, high deposition efficiencies can be achieved by mixing nitrogen with He or by using only He as the process gas. SEM images of the microstructure of a MCrAlY coating are shown in Fig. 9. This coating was produced with He to achieve a particle impact velocity of about 1000 m/s for a 10 μm diameter particle. The shape of the particles has changed little in the spray process. Intensive plastic deformation is concentrated in a very thin layer at the surface of the particles. A model of the deformation process during the particle impact on the substrate or the coating by Assadi et al.[12] has shown that the surface of the particles in the contact zone can possibly heat to the melting temperature during the impact process.

Costs for the cold spray process are comparable to that of HVOF spraying, but cold spray is especially suitable for spraying of metallic materials. It has the advantage that very dense coatings of low oxide content can be produced and even very oxidation-sensitive materials can be used. The thermal stresses on the spray and substrate material are minimal because of the low temperature of the process. It is possible to produce coatings and structures that are several centimeters thick. The free jet from the spray is only a few millimeters in diameter, thus very complex geometries can be sprayed, and masking of those components that should not be coated might not be necessary.

7. Summary

Cold spraying is a significant addition to the plethora of established thermal spray processes and offers new applications for spray technology. It makes it possible to produce metal coatings with very little porosity and oxygen content. This is advantageous for the physical properties such as the electrical conductivity and for corrosion resistance.

The process does not require any melting of the spray material, but the microstructure of the coatings indicates that the plastic deformation of the particles upon impact causes significant heating limited to a thin layer at the particle surface, which can reach the melting point. Adhesion occurs if the particles have a certain critical impact velocity, which is a function of the spray material and its plastic deformation characteristics.

The particle temperatures and velocities achieved in a cold

spray device can be evaluated for different nozzle geometries and gas process parameters with CFD. Such computations offer the possibility to evaluate optimal spray conditions with little experimental effort.

To optimize the spray conditions for a given powder, the deposition efficiency has to be determined experimentally for only one set of parameters. On the basis of the concept of a critical velocity, the deposition efficiency can then be calculated for other nozzle geometries, process gases, and parameter settings with a CFD program. This also allows a decision about whether He, nitrogen, or a mixture thereof is needed to achieve a required deposition efficiency.

Acknowledgments

The authors would like to thank P. Heinrich and W. Kroemmer from Linde Gas AG for technical support in building the cold spray apparatus and for providing the gas for the experiments.

References

1. A.P. Alkhimov, A.N. Papyrin, V.F. Kosarev, N.I. Nesterovich, and M.M. Shushpanov: "Gas-Dynamic Spray Method for Applying a Coating," U.S. Patent 5 302 414, 12 Apr, 1994.
2. A.P. Alkhimov, A.N. Papyrin, V.F. Kosarev, N.I. Nesterovich, and M.M. Shushpanov: "Method and Device for Coating," European Patent 0 484 533 B1, 25 Jan, 1995.
3. R.C. McCune, A.N. Papyrin, J.N. Hall W.L. Riggs II, and P.H. Zajchowski: "An Exploration of the Cold-Gas-Dynamic Spray Method for Several Materials Systems" in *Advances in Thermal Spray Science and Technology, Proceedings of the 8th National Thermal Spray Conference,* C.C. Berndt and S. Sampath, ed., ASM International, Materials Park, OH, 1995, pp. 1-5.
4. V.V. Sychev, A.A. Vasserman, A.D. Kozlov, G.A. Spiridonov, and V.A. Tsymarny: *Thermodynamic Properties of Nitrogen,* Hemisphere Publishing Corporation, Washington, DC, 1987.
5. V.V. Sychev, A.A. Vasserman, A.D. Kozlov, G.A. Spiridonov, and V.A. Tsymarny: *Thermodynamic Properties of Helium,* Hemisphere Publishing Corporation, Washington, DC, 1987.
6. G.B. Wallis: *One-Dimensional Two-Phase-Flow,* McGraw Hill, New York, 1969.
7. J.M. Walsh: "Drag Coefficient Equation for Small Particles in High Speed Flows," *AIAA J.,* 1975, *13*(11), pp. 1526-28.
8. U. Meingast: "Investigations and Thermodynamic Aspects of Thermal Spray Processes and Fluid-Dynamic Computations of HVOF Spray Devices," Master's Thesis, Thayer School of Engineering, Dartmouth College, and RWTH Aachen, Germany, 1997.
9. C. Borchers, T. Stoltenhoff, F. Gärtner, and H. Kreye: "Deformation Microstructure of Cold Sprayed Coatings Studied by Electron Microscopy," MRS Spring Meeting, San Francisco, CA, 2001.
10. R.C. McCune, W.T. Donlon, O.O. Popoola, and E.L. Cartwright: "Characterization of Copper Layers Produced by Cold Gas-Dynamic Spraying," *J. Therm. Spray Technol.,* 2000, *9*(1), 73-82.
11. H. Kreye, M. Hammerschmidt, U. Granz, and C.-P. Woidneck: Über den Bindemechanismus beim Explosivschweißen, *Schweissen Schneiden,* 1985, *37,* 297-302 (in German).
12. H. Assadi, F. Gärtner, T. Stoltenhoff, and H. Kreye: Cold Gas Spraying—Modelling of Particle Impact, *Acta Mater.,* in press.